AMERICAN SOCIETY FOR MICROBIOLOGY | Journal of Virology®

VIRUS-CELL INTERACTIONS

Herpes Simplex Virus 1 Expressing GFP-Tagged Virion Host Shutoff (vhs) Protein Uncouples the Activities of RNA Degradation and Differential Nuclear Retention of the Virus Transcriptome

Emma L. Wise,[a] Jerzy Samolej,[a*] Gillian Elliott[a]

[a]Section of Virology, Department of Microbial Sciences, Faculty of Health and Medical Sciences, University of Surrey, Guildford, Surrey, United Kingdom

ABSTRACT Virion host shutoff (vhs) protein is an endoribonuclease encoded by herpes simplex virus 1 (HSV1). vhs causes several changes to the infected cell environment that favor the translation of late (L) virus proteins: cellular mRNAs are degraded, immediate early (IE) and early (E) viral transcripts are sequestered in the nucleus with polyA binding protein (PABPC1), and dsRNA is degraded to help dampen the PKR-dependent stress response. To further our understanding of the cell biology of vhs, we constructed a virus expressing vhs tagged at its C terminus with GFP. When first expressed, vhs-GFP localized to juxtanuclear clusters, and later it colocalized and interacted with its binding partner VP16, and was packaged into virions. Despite vhs-GFP maintaining activity when expressed in isolation, it failed to degrade mRNA or relocalise PABPC1 during infection, while viral transcript levels were similar to those seen for a vhs knockout virus. PKR phosphorylation was also enhanced in vhs-GFP infected cells, which is in line with a failure to degrade dsRNA. Nonetheless, mRNA FISH revealed that as in Wt but not Dvhs infection, IE and E, but not L transcripts were retained in the nucleus of vhs-GFP infected cells at late times. These results revealed that the vhs-induced nuclear retention of IE and E transcripts was dependent on vhs expression but not on its endoribonuclease activity, uncoupling these two functions of vhs.

IMPORTANCE Like many viruses, herpes simplex virus 1 (HSV1) expresses an endoribonuclease, the virion host shutoff (vhs) protein, which regulates the RNA environment of the infected cell and facilitates the classical cascade of virus protein translation. It does this by causing the degradation of some mRNA molecules and the nuclear retention of others. Here, we describe a virus expressing vhs tagged at its C terminus with a green fluorescent protein (GFP) and show that the vhs-GFP fusion protein retains the physical properties of native vhs but does not induce the degradation of mRNA. Nonetheless, vhs-GFP maintains the ability to trap the early virus transcriptome in the nucleus to favor late protein translation, proving for the first time that mRNA degradation is not a prerequisite for vhs effects on the nuclear transcriptome. This virus, therefore, has uncoupled the nuclear retention and degradation activities of vhs, providing a new understanding of vhs during infection.

KEYWORDS GFP, PABPC1, endoribonuclease, nuclear retention, virion host shutoff

The UL41 gene of herpes simplex virus 1 (HSV-1) encodes the virion host shutoff (vhs) protein, an important virulence factor that is conserved across the alphaherpesvirinae sub-family (1). vhs is an endoribonuclease that induces the degradation of mRNA, but not rRNA or tRNA (2–4), by binding to the cellular translation initiation machinery through the eIF4A and eIF4H components of the eIF4F cap-binding complex, resulting in mRNA cleavage (1, 5–7). This activity effectively shuts down cellular protein synthesis (8, 9), freeing up ribosomes

Editor Lori Frappier, University of Toronto

Address correspondence to Gillian Elliott, g.elliott@surrey.ac.uk.

*Present address: Jerzy Samolej, Institute of Microbiology and Infection, University of Birmingham, Birmingham, United Kingdom.

The authors declare no conflict of interest.

Received 31 December 2021
Accepted 23 May 2022
Published 27 June 2022

to translate viral mRNA. One consequence of vhs activity is that cellular transcripts encoding interferon-stimulated genes (ISGs), generated in response to virus infection, are targeted for degradation, thereby blunting the host's innate response (10, 11). More recently, vhs has also been shown to induce the degradation of double-stranded RNA contributing to the inhibition of the protein kinase R (PKR) response in virus infection and revealing an additional role for vhs in counteracting host defenses (12).

In theory, vhs should target all translating transcripts equally, both host and viral. However, transcriptomic analyses from our group have demonstrated that cellular mRNAs exhibit a wide range of susceptibility to vhs activity, ranging from almost complete resistance to 1000-fold reduction, suggesting that specificity for vhs activity exists (10). This result was also confirmed in another recent study (13). In the case of virus transcripts, vhs has been shown to play a key role in regulating viral gene expression during the classical herpesvirus cascade by reducing the levels of immediate early (IE) and early (E) viral transcripts at the transition to late (L) gene expression (2, 14). In addition, previous work from our group has revealed a novel mechanism whereby vhs causes the nuclear retention of mRNAs, providing an alternative mechanism of translation inhibition (10, 15). mRNA FISH was used to show that IE and E transcripts were retained in the nucleus in a vhs-dependent fashion from around 10 h onwards, whereas L transcripts were effectively exported to the cytoplasm (15). In the absence of vhs, all viral transcripts were cytoplasmic.

Concomitant with this nuclear retention of mRNA, the steady-state localization of the polyA binding proteins PABPC1 is altered from cytoplasmic to nuclear in HSV1 infected cells (10, 15, 16). PABPC1 binds the polyA tails of mRNA transcripts in the nucleus and shuttles between the nucleus and cytoplasm as mRNAs undergo nuclear export, translation, and normal cellular degradation (17, 18). In uninfected cells, PABPC1 has a steady-state cytoplasmic localization, however upon infection with HSV-1, or expression of vhs by transient transfection, PABPC1 accumulates in the nucleus in a vhs-dependant manner (10, 15), meaning that relative PABPC1 localization is a useful surrogate for vhs function. These observations follow those seen previously for the Kaposi's sarcoma herpesvirus (KSHV) SOX protein (19, 20), revealing the potential for a universal mechanism across the herpesviruses for regulating RNA metabolism.

Given its profound activity on the cellular transcriptome, vhs would be expected to be lethal to the virus if left unchecked. In recent years it has become clear that the virus uses several mechanisms to lessen the consequences of vhs activity. First, when expressed in isolation by transient transfection, vhs protein fails to accumulate (15, 21), a feature which has been attributed in part to the presence of transferable inhibitory sequences within the mRNA (15). Second, the vhs transcript itself is predominantly localized in the nucleus when expressed during virus infection or in isolation, providing another layer of translation inhibition (15). A third process for regulating vhs activity in virus infection is through the formation of a trimeric complex between the vhs protein and the viral proteins VP16 and VP22 (15, 21) in which VP16 binds directly to vhs (22) and VP22 binds directly to VP16 (23). The formation of this complex not only blocks vhs activity but rescues its expression compared to the level expressed during transfection (10, 21). As such, both VP16 and VP22 deletion viruses exhibit profound shutoff of translation in the infected cell but paradoxically express a much lower level of vhs protein (10, 24–26), while Δ22 viruses are rescued by spontaneous mutations in vhs (10, 24, 27). This originally led to the hypothesis that vhs endoribonuclease activity is overactive in the absence of VP22, but our recent work has shown that the main outcome of deleting VP22 is not increased mRNA degradation *per se* but increased nuclear retention of the viral transcriptome (10). As such, the nuclear export of L transcripts and subsequent late protein synthesis was dependent on the presence of VP22 (10).

To date, our cell biological studies of vhs have been impeded by the lack of an effective anti-vhs antibody for downstream studies. Here we report the generation and characterization of a recombinant HSV1 which expresses vhs tagged with GFP at its C- terminus (vhs-GFP). We show that HSV1 vhs-GFP maintains many characteristics of the wild-type (WT) virus, including similar plaque size, viral gene expression, the ability to form a complex with VP16

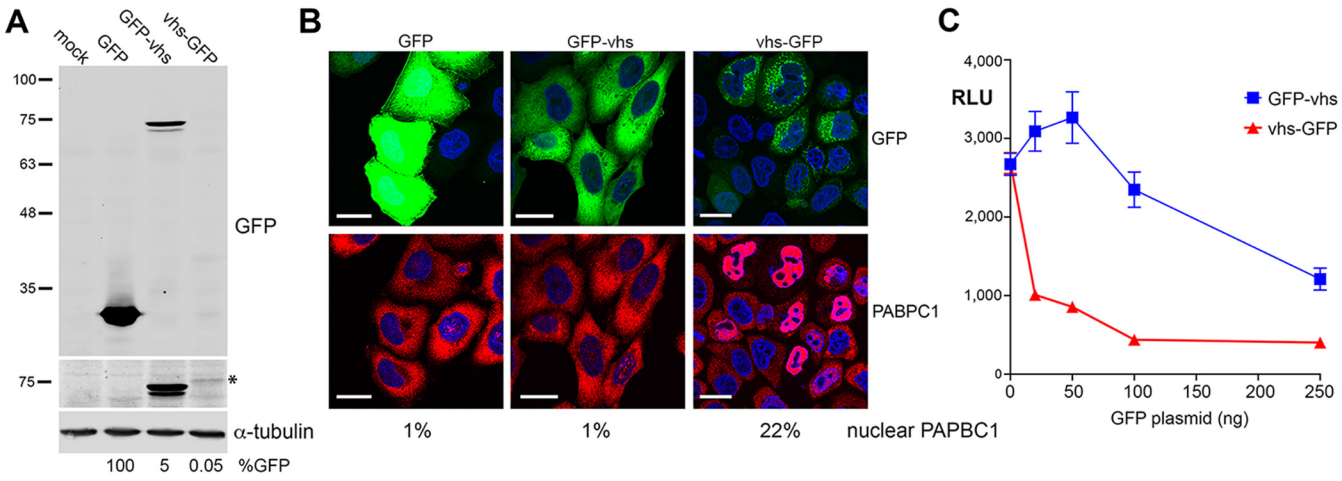

FIG 1 Characterization of GFP-tagged vhs proteins. (A) HeLa cells were mock-transfected or transfected with plasmids expressing GFP-tagged proteins as shown. After 20 h, total cell lysates were analyzed by Western blotting for GFP and α-tubulin. Relative expression of GFP was quantitated using LICOR ImageStudio and is represented as a percentage of untagged GFP level, normalized to tubulin (B). (A) Transfected cells grown on coverslips were fixed and stained for PABPC1 (red) and nuclei stained with DAPI (blue). Scale bar = 20 μm. The percentage of cells in the monolayer with nuclear PABPC1 is shown (>200 cells counted). (C) HeLa cells grown in 24-well plates were transfected with 50 ng plasmid expressing Gaussia luciferase, together with increasing amounts of a plasmid expressing either GFP-vhs or vhs-GFP. After 16 h, the medium was changed and 6 h later the medium was sampled, and relative luciferase levels were measured by injection of coelenterazine in a Clariostar plate reader. The means $\pm$ standard errors of the means (SEM) for one representative experiment are shown (n = 4). RLU, relative light units (arbitrary).

and VP22, and virion packaging of vhs itself. We also show that when first expressed, vhs-GFP concentrates in a juxtanuclear position in close proximity to but not associated with the Golgi apparatus, while later in infection it co-localises with VP16. Despite the vhs-GFP retaining activity in transient transfection, it failed to induce mRNA degradation or PABPC1 relocalization to the nucleus in the context of virus infection, whereas PKR phosphorylation was enhanced, suggesting that vhs enzymatic activity was abrogated in this virus. Nonetheless, mRNA FISH of virus transcripts revealed that nuclear retention of IE and E mRNA was maintained in cells infected with HSV1 vhs-GFP, despite a lack of mRNA degradation. This unexpected result uncoupled the endoribonuclease and nuclear retention activities of vhs, providing us with a unique tool to investigate these discrete molecular aspects of vhs function.

RESULTS

Vhs tagged with GFP at its C terminus retained endoribonuclease activity. To determine if vhs retains activity when fused to GFP, we first tagged vhs at either its N or C terminus and expressed it by transient transfection in HeLa cells. Total protein analyzed by SDS-PAGE and Western blotting for GFP revealed that, as expected, GFP accumulated to high levels in transfected cells, but GFP-vhs was around 20-fold lower, while expression of vhs-GFP was 2,000-fold lower (Fig. 1A). These results were in line with previous experiments by us and others where it was shown that vhs protein failed to accumulate during transient transfection despite vhs mRNA levels being similar to those in infected cells (1, 15, 21).

The ability of GFP-vhs or vhs-GFP to relocalize PABPC1 to the nucleus of HeLa cells, which was taken as being indicative of endoribonuclease activity, was measured using immunofluorescence of PABPC1. Following transfection with a plasmid expressing GFP alone, PABPC1 remained cytoplasmic (Fig. 1B). However, while vhs-GFP caused PABPC1 relocalization to the nucleus, GFP-vhs failed to do so, indicating that vhs functionality was retained only in vhs tagged at its C terminus with GFP (Fig. 1B). This was further confirmed by cotransfection of HeLa cells with a plasmid expressing the reporter Gaussia Luciferase (GauLuc) and increasing amounts of a plasmid expressing either GFP-vhs or vhs-GFP. Measurement of GauLuc secreted into the cell medium indicated that co-expression of vhs-GFP but not GFP-vhs caused a drop in GauLuc expression at low levels of vhs-GFP plasmid (Fig. 1C). Furthermore, mRNA FISH using a probe for GFP indicated that, while the GFP and GFP-vhs transcripts were localized in the cytoplasm, the vhs-GFP transcript was retained in the nucleus (Fig. 2).

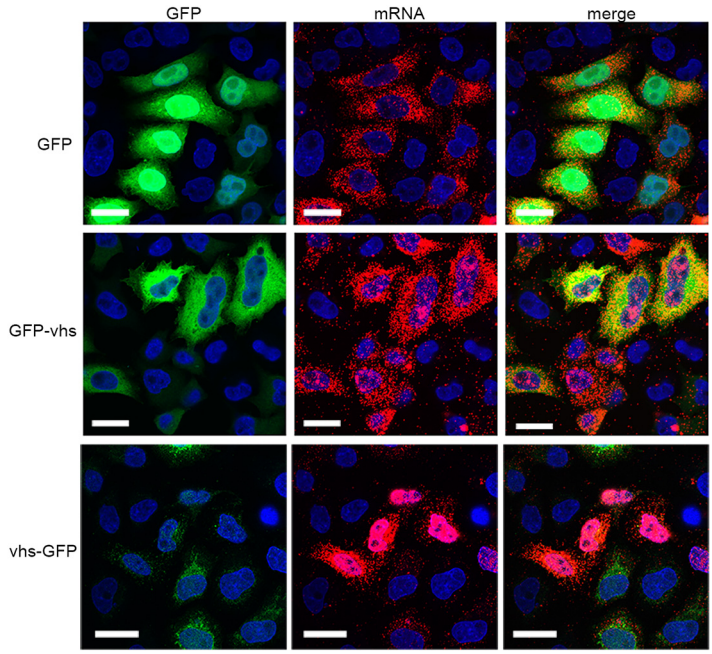

FIG 2 Nuclear localization of the vhs-GFP transcript in transfected cells. HeLa cells grown in two-well chamber slides were transfected with plasmids expressing GFP-tagged proteins as shown, and after 20 h were fixed in 4% paraformaldehyde. Cells were then processed for mRNA FISH using a GFP-specific probe (red) and nuclei stained with DAPI (blue). GFP is in green. Scale bar = 20 μm.

This confirmed that, unlike GFP-vhs, vhs-GFP seemed to retain the full characteristics of the native vhs transcript (15).

Characterization of recombinant HSV1 expressing a vhs-GFP fusion protein. A recombinant HSV1 in strain Sc16 was subsequently generated using homologous recombination to express vhs-GFP in place of vhs (Fig. 3A). Following three rounds of plaque purification on Vero cells, vhs-GFP expression was confirmed by analyzing total infected cell protein by SDS-PAGE and Western blotting for GFP, vhs, and a loading control of α-tubulin (Fig. 3B). Another recombinant virus expressing a different tagged protein, YFP-UL47, was analyzed simultaneously to directly compare the relative expression of vhs with a second tagged virus protein (Fig. 3B). In HSV1 vhs-GFP infected cells, a protein band of the correct size was detected with both the vhs and the GFP antibodies, confirming the expression of vhs-GFP in this virus (Fig. 3B). Moreover, while the vhs antibody indicated that vhs was detected at slightly lower levels in vhs-GFP than in WT or YFP-UL47 infected cells, quantification of the respective vhs-GFP and YFP-UL47 bands using the GFP antibody (which detects YFP with equal efficiency) indicated that vhs was expressed at a level 14-fold lower than UL47, reenforcing the relatively poor expression of vhs in comparison to another tegument protein (Fig. 3B). Plaque assays on Vero and human foetal foreskin fibroblast (HFFF) cells further indicated that the plaque size of HSV1 vhs-GFP was similar to that of the WT Sc16 virus suggesting that virus replication was not significantly impaired by the expression of vhs-GFP in place of vhs (Fig. 3C). The growth characteristics of vhs-GFP were next compared to that of WT strain Sc16 in a single-step growth curve in HFFF cells. Cells were infected at a multiplicity of infection (MOI) of 2 and the total virus was harvested every 5 h up to 30 h, and titrated on Vero cells, indicating that vhs-GFP replication was delayed by around 5 h compared to WT virus but ultimately reached approximately the same titer (Fig. 3D). A similar infection time course was analyzed for protein expression by SDS-PAGE and Western blotting to assess the kinetics of expression of representative viral proteins (Fig. 3E). Blotting for ICP27, TK, and VP16, representative of the viral gene classes IE, E, and L respectively, showed that the kinetics of expression of all three classes was similar between WT and HSV1 vhs-GFP infections, while vhs and GFP blots confirmed the expression of vhs-GFP with similar kinetics to vhs alone (Fig. 3E). Although quantification of the 20 h

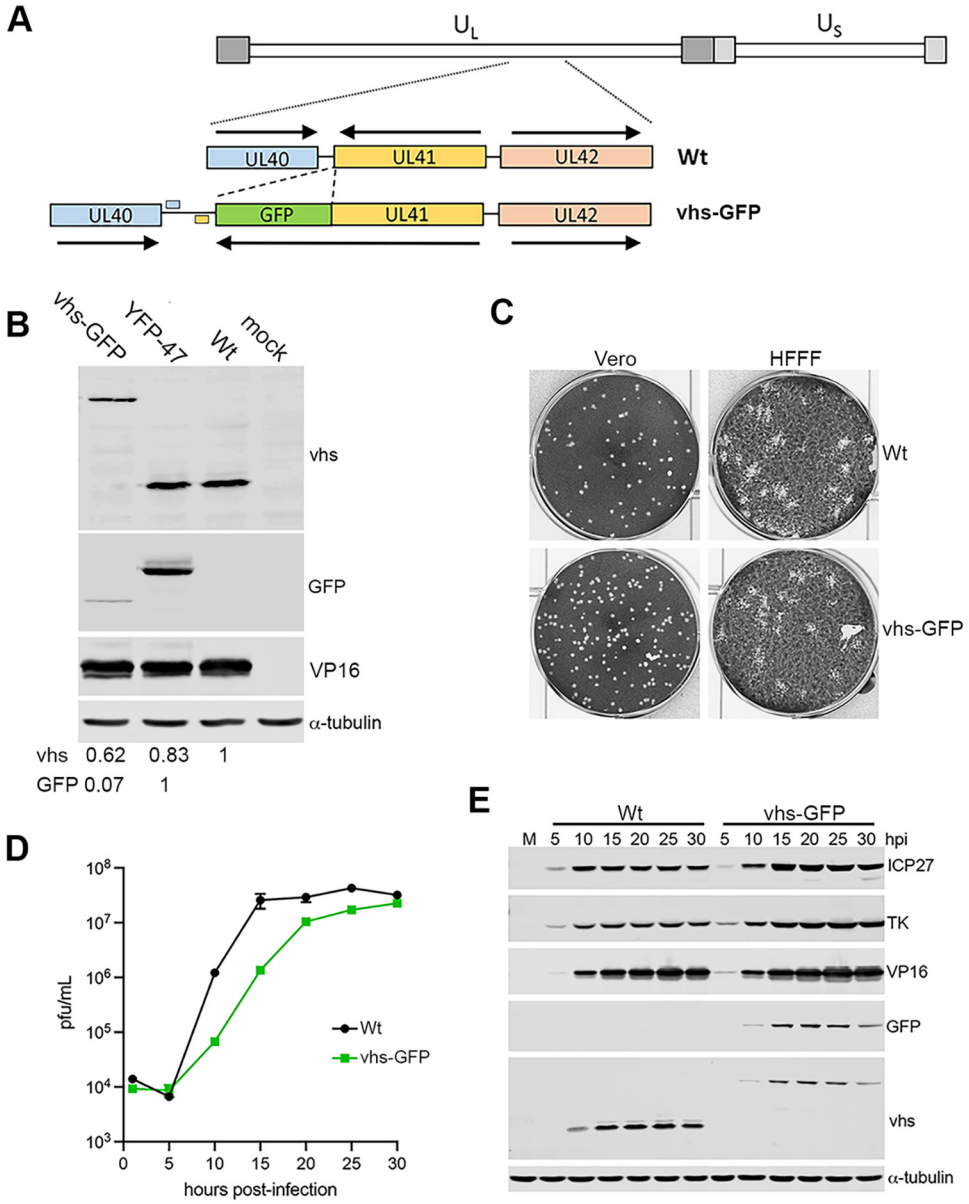

FIG 3 Construction and characterization of HSV1 expressing vhs-GFP. (A) HSV1 expressing vhs-GFP in place of GFP was constructed by cotransfecting Vero cells with infectious Sc16 genomic DNA and a plasmid containing the UL41GFP fusion gene surrounded by the flanking sequences from UL40 and UL42. Polyadenylation signals for UL40 and UL41 are shown. (B) HFFF cells were mock-infected or infected with Sc16, plaque purified vhs-GFP or YFP-UL47 viruses at an MOI of 2, and total protein harvested at 16 hpi before separation by SDS-PAGE and Western blotting with antibodies for GFP, vhs, VP16, and α-tubulin. Relative expression of vhs and GFP were quantitated using LI-COR ImageStudio and normalized to α-tubulin. (C) Vero and HFFF cells were infected with around 40 PFU of Sc16 or vhs-GFP and incubated for 3 days before fixation and staining with crystal violet. (D) One-step growth curves for WT (Sc16) and HSV1 vhs-GFP viruses were carried out by harvesting the total virus from HFFF cells infected at an MOI of 2 every 5 h up to 30 h. Samples were titrated onto Vero cells. The mean titer of three replicates and associated SEM are plotted. (E) Total extracts of HFFF cells infected as in (D) were analyzed by SDS-PAGE and Western blotting for the indicated virus proteins and α-tubulin as a loading control.

samples indicated around 2-fold less vhs present in the vhs-GFP expressing cells compared to vhs-expressing cells, it should be noted that the increased molecular weight of the GFP fusion and hence potentially less efficient transfer to the membrane might contribute to this reduction.

To investigate where vhs localizes in the infected cell, HFFF cells infected with HSV1 vhs-GFP were fixed at various times after infection and imaged for GFP fluorescence using confocal microscopy. In line with Western blotting, vhs-GFP was first detected at low

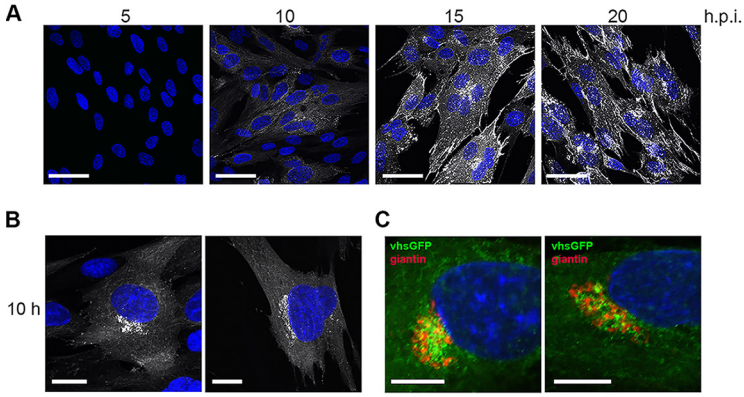

FIG 4 Localization of vhs-GFP during HSV1 infection. (A) HFFF cells infected with HSV1 vhs-GFP at an MOI of 2 were fixed at the indicated times, stained with DAPI (blue), and imaged for GFP fluorescence (white) using confocal microscopy. Scale bar = 50 μm. (B) Examples of the 10 h sample from (A) imaged at higher magnification. Scale bar = 20 μm. (C) HFFF cells infected as in (A) were fixed and stained for the Golgi marker giantin. Scale bar = 10 μm.

levels at around 10 h and increased in intensity to 15 h, when it was particularly concentrated close to the nucleus and at the cell periphery (Fig. 4A). Closer examination of the 10-h sample revealed that vhs-GFP was clustered in a juxtanuclear location when first expressed at detectable levels (Fig. 4B), but the staining of cells at this time with an antibody for giantin, which localizes the cis/medial Golgi indicated that these clusters, while in the proximity of the Golgi apparatus, did not colocalize with giantin (Fig. 4C).

The vhs-GFP fusion protein maintained the ability to form the vhs-VP16-VP22 complex in infected cells. Viral protein VP16 binds directly to vhs, and together with VP22 regulates the activity of vhs (22, 26). Immunofluorescence of VP16 in HSV1 vhs-GFP infected cells indicated that these two proteins were extensively colocalized in close to 100% of infected cells at later times in infection when virus assembly would be optimal (Fig. 5A). To determine if vhs-GFP interacted with VP16 and VP22 during infection, a GFP-TRAP pulldown was performed on extracts of HaCat cells infected with either vhs-GFP or WT viruses at an MOI of 5, harvested at 24 h. The resulting pulldown complex was analyzed by Western blotting, indicating that both VP16 and VP22 were present in the vhs-GFP interactome but not the pulldown from WT infected cells, while the virus protein UL16, used as a negative-control, was absent from both (Fig. 5B). This suggested that the vhs-GFP fusion protein was capable of binding its usual viral protein partners.

The interaction between VP16 and vhs has also been implicated in the packaging of vhs into the virion (22). To test the assembly of vhs-GFP, extracellular HSV1 vhs-GFP and WT virions were purified from infected HaCat cells by centrifuging on a 5% to 15% Ficoll gradient. Solubilized virions were analyzed by SDS-PAGE followed by Coomassie blue staining and Western blotting (Fig. 5C and D). Using the VP5 major capsid protein band to equalize virion loading, the total protein profiles for each virus were determined to be comparable (Fig. 5C). Western blotting for viral proteins vhs, GFP, VP16, and VP22, using VP5 as a loading control confirmed the presence of the ~55 kDa vhs protein in WT virions and the ~82 kDa fusion protein in vhs-GFP virions (Fig. 5D). Although VP16 was equally packaged in both virion samples, vhs-GFP was present around 5-fold lower than WT vhs (Fig. 5D) suggesting that packaging of vhs-GFP into virions may be less efficient than WT virus.

vhs-GFP lacked endoribonuclease activity in infected cells. We previously showed that PABPC1 was relocalized from the cytoplasm to the nucleus in a vhs-dependent manner in both HSV1 infected cells and cells transfected with a plasmid expressing vhs (22). During the initial transfection experiments, we also showed that when transfected into HeLa cells, vhs-GFP was also capable of relocalizing PABPC1 to the nucleus (Fig. 1B). To confirm that this activity was maintained in HSV1 vhs-GFP, HFFF cells infected with either WT or HSV1 vhs-GFP were fixed at 16 h and stained for PABPC1. As shown previously, PABPC1 was concentrated in nuclear accumulations in WT infected cells (Fig. 6). By contrast, PABPC1 remained cytoplasmic

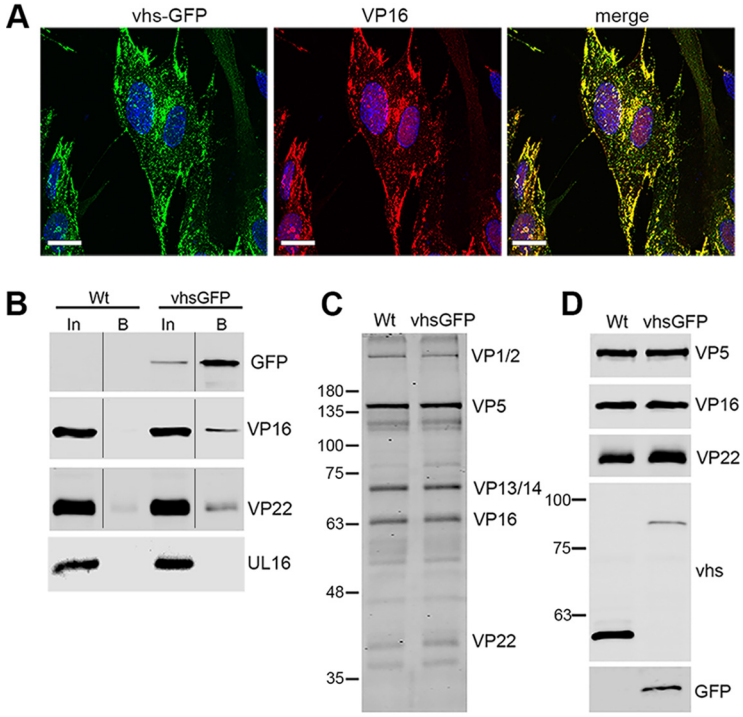

FIG 5 Interaction of vhs-GFP with VP16 and assembly into virions. (A) HFFF cells infected with HSV1 vhs-GFP at an MOI of 2 were fixed at 16 h, stained for VP16 (red), and imaged for GFP (green). Nuclei were stained with DAPI (blue). Scale bar = 20 μm. (B) GFP-Trap pulldown was carried out on HaCat cells infected with WT (Sc16) or vhs-GFP at an MOI of 5 and harvested at 24 hpi. The pulldowns were analyzed by SDS-PAGE and Western blotting with antibodies to GFP, VP16 and VP22, and UL16 as a control for nonspecific pulldown of virus protein. In = input, B = pulldown (C and D) Extracellular virions were purified on 5% to 15% Ficoll gradients and analyzed by SDS-PAGE followed by Coomassie blue staining (C) or Western blotting with antibodies as indicated (D).

in HSV1 vhs-GFP infected cells even as late as 20 h after infection (Fig. 6). Moreover, a second independently-isolated recombinant virus expressing vhs-GFP also failed to relocalize PABPC1, confirming that this result was a consequence of expressing vhs as a GFP fusion protein in the virus (unpublished data).

The lack of PABPC1 relocalization to the nucleus raised the possibility that vhs may not be active as an endoribonuclease when expressed in the context of virus infection. To test the ability of the vhs-GFP fusion protein to degrade cellular mRNA, relative levels of two ISG transcripts (IFIT1 and IFIT2) and two transcripts previously shown to be hypersensitive to vhs activity (MMP1 and MMP3) were measured by RT-qPCR at 16 h. IFIT1 transcript was reduced, while IFIT2 was unchanged in WT infection compared to mock-infected control (Fig. 7A) as shown in our previous work (10). By contrast, these ISG transcripts were both upregulated in HSV1 vhs-GFP infection by around $\log_2$ change of 3, suggesting that these transcripts were not degraded by vhs-GFP and were being activated in response to virus infection, as shown previously in cells infected with a vhs knockout virus (10). In the case of MMP1 and MMP3, these transcripts were reduced by $\log_2$ change of 8 in WT infection, again as shown previously (10), but these transcripts were only slightly reduced in the HSV1 vhs-GFP infection compared to the mock-infected control at 16 h (Fig. 7A). For all four transcripts, very similar results were observed at 24 h to those at 16 h, suggesting that the ability of vhs-GFP to degrade cellular transcripts was impaired, rather than delayed.

Viral transcripts representing IE (ICP22), E (TK), and L (gC) genes were measured in the same way as the cellular transcripts, but in this case, the $\log_2$ change was compared to WT infected cells. ICP22 and TK transcripts were significantly more abundant in HSV1 vhs-GFP infection compared to WT (Fig. 7B), but the level of the late gC transcript was not significantly different between the two viruses, which was in agreement with our previous results on Δvhs infected cells (10). Hence, the significant differences in IE and E mRNA transcript levels

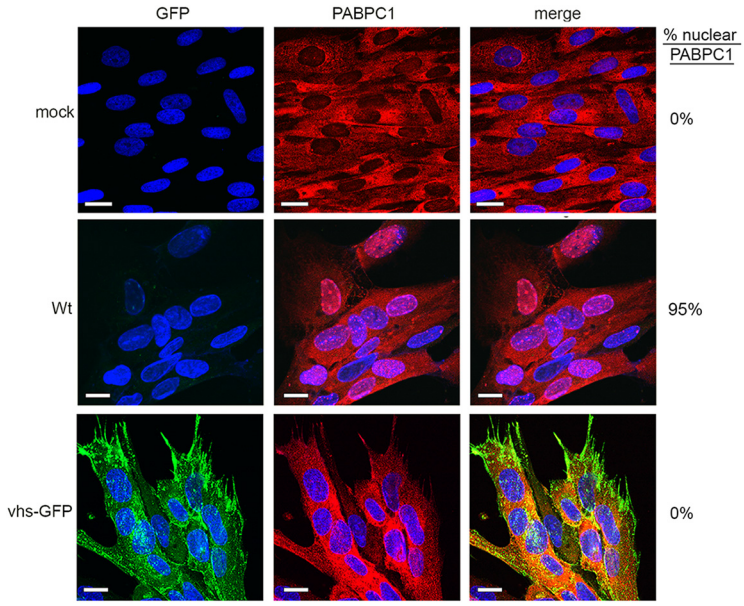

FIG 6 PABPC1 is not relocalized in HSV1 vhs-GFP infection. HFFF cells infected with WT (Sc16) or HSV1 vhs-GFP viruses at an MOI of 2 were fixed at 16 h, stained with an antibody for PABPC1 (red), and nuclei stained with DAPI (blue). Scale bar = 20 μm. Percentage cells in the monolayer with nuclear PABPC1 are shown on the right-hand side.

between HSV1 vhs-GFP and WT infection further suggested that the vhs-GFP fusion protein was severely impaired or non-functional with respect to its mRNA degradation capabilities. Although vhs expression itself was shown to be reduced by 2-fold in HSV1 vhs-GFP infected cells (Fig. 3), this reduction was not enough to account for the absence of mRNA degradation described here.

Another consequence of vhs endoribonuclease activity is the degradation of double-stranded RNA formed by the annealing of virus mRNA transcribed from both strands of the virus genome, thereby contributing to the suppression of PKR phosphorylation and subsequent eIF2α phosphorylation in infected cells to counteract translational shutoff (12). This suggests that vhs acts in tandem with two other virus factors: Us11, which blocks PKR phosphorylation (28), and ICP34.5, which controls eIF2α phosphorylation (29). Western blotting of WT and HSV1 vhs-GFP infected cell extracts indicated that PKR phosphorylation was indeed enhanced in cells expressing vhs-GFP compared to WT virus infection (Fig. 7C). Increased PKR phosphorylation was also reflected in an increase in eIF2α phosphorylation in HSV1 vhs-GFP infection.

Nuclear retention of the infected cell transcriptome in HSV1 vhs-GFP infected cells. The failure of vhs-GFP to degrade infected cell mRNA led us to hypothesize that this virus would be equivalent to a Δvhs virus in that all vhs activities would be abrogated by the fusion of GFP at its C terminus in the context of virus infection. Because we had not yet formally shown that vhs endoribonuclease activity was required for the nuclear retention of the infected cell transcriptome (10, 15), mRNA FISH was carried out on infected HFFF cells for representative IE (ICP27) E (TK), and L (gD) transcripts. WT infected cells recapitulated our previous results that IE and E transcripts but not L transcripts were retained in the nucleus at later times of infection (Fig. 8A, WT), but in Δvhs infected cells, all classes of the transcript were entirely cytoplasmic, thereby confirming that vhs was required for nuclear retention of these transcripts (Fig. 8A, Δvhs). However, in the HSV1 vhs-GFP infected cells, IE and E transcripts were also retained in the nucleus (Fig. 8A, vhs-GFP), despite vhs-GFP failing to induce the degradation of mRNA or the nuclear retention of PABPC1. Finally, the localization of the vhs-GFP transcript itself was examined in infected cells using a probe for GFP or vhs. This revealed that for WT infection where the vhs transcript was predominantly nuclear, the vhs-GFP transcript was also retained in the nucleus (Fig. 8C), confirming the results obtained above in cells expressing vhs-GFP by transfection.

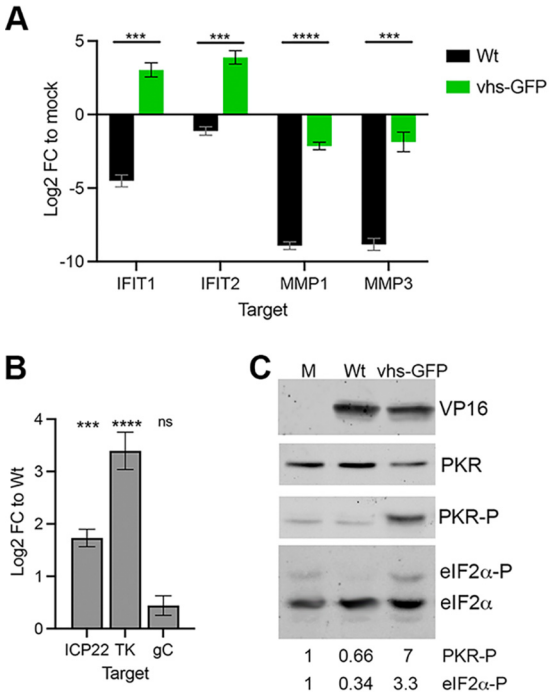

FIG 7 vhs-GFP expressed in virus infection is deficient in endoribonuclease activity. (A) HFFF cells were infected with WT or HSV1 vhs-GFP viruses at an MOI of 5. Total RNA was purified at 16 hpi and subjected to RT-qPCR for cellular transcripts previously identified as being susceptible to vhs activity. The mean and ± standard error for $n = 3$ is shown. Statistical analysis was carried out using an unpaired *t* test. ***, $P < 0.001$; ****, $P < 0.0001$. (B) RNA samples from (A) were subjected to RT-qPCR of viral transcripts ICP22 (IE), TK (E), and gC (L). The mean and ± standard error for $n = 3$ is shown. Statistical analysis was carried out using an unpaired *t* test. ***, $P < 0.001$; ****, $P < 0.0001$; ns, not significant. (C) HFFF cells infected with WT or HSV1 vhs-GFP viruses at MOI of 2 were harvested at 16 h and analyzed by SDS-PAGE and Western blotting with antibodies as indicated. Western blotting for eIF2α was carried out using 10 μm Phos-tag PAGE. The relative level of phospho-PKR and phospho-eIF2α was quantitated using LI-COR Image Studio and is represented relative to the level in uninfected cells.

These unexpected results indicated that, although vhs-GFP lacks endoribonuclease activity in HSV1 infected cells, it retained the ability to alter the compartmentalization of the infected cell transcriptome, both viral and cellular. Hence, these two properties of vhs were uncoupled in the HSV1 vhs-GFP virus, providing scope for the further molecular understanding of vhs activity.

DISCUSSION

The vhs protein of HSV1 is involved in regulating the RNA environment of the infected cell. Not only does it induce the degradation of mRNA and dsRNA (3, 4, 12), but it also causes the nuclear retention of both the viral and the cellular transcriptome (10). The overall effect of this activity is to enhance the translation of the late virus transcriptome not only by sequestration of the early virus transcriptome in the nucleus but also by reducing the PKR stress response (12, 30). As a virulence factor, vhs, therefore, helps to optimize the virus infection process and block the establishment of an antiviral environment in the cell. In this study we aimed to develop a cell biology tool for studying vhs, using a vhs-GFP fusion protein that had been demonstrated to function when expressed in isolation. Surprisingly, we found that vhs-GFP exhibited little if any endoribonuclease activity despite functioning in isolation and maintaining its physical characteristics during infection, a result that was backed up by the failure of PABPC1 to relocalize to the nucleus. This suggests that the addition of GFP to the C terminus of vhs differentially affects its activity depending on whether it is expressed in isolation or virus infection. Although the reason for this is not yet clear, it points to the fact that vhs endoribonuclease activity during infection is a complex process that is

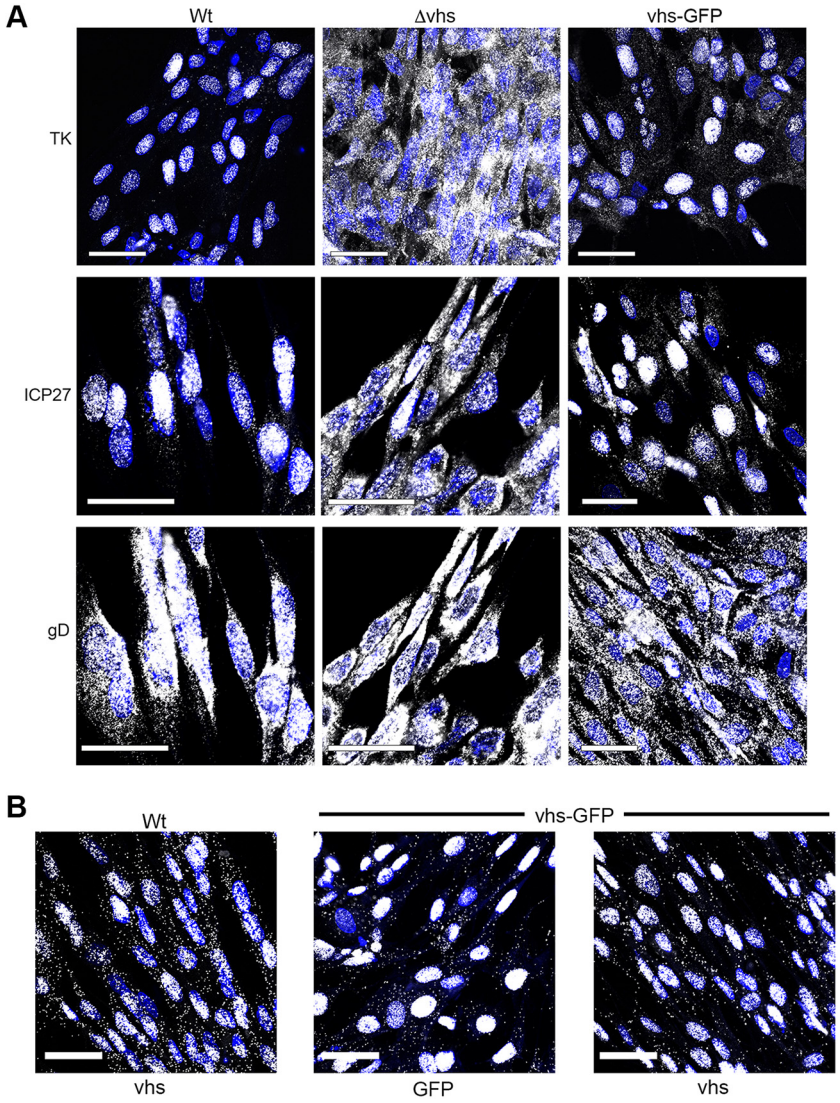

FIG 8 vhs-GFP maintains the ability to cause the nuclear retention of viral transcripts. (A) HFFF cells grown in two-well slide chambers were infected with WT, Δvhs, or HSV1 vhs-GFP at an MOI of 2 and fixed after 16 h in 4% paraformaldehyde. Cells were then processed for mRNA FISH using probes specific for IE (ICP27), E (TK), and L (gD) transcripts (all in white). Note, that the same field in WT and Δvhs infection is shown for ICP27 and gD mRNA FISH. (B) As above but WT or HSV1 vhs-GFP infected cells were stained with a probe for UL41 or GFP (in white). Nuclei were stained with DAPI (blue). Scale bar = 50 μm.

not reflected in vhs expression alone. The GFP moiety may block the binding of additional partners required for full activity during infection.

The very low level of vhs-GFP protein, when expressed in isolation, was not unexpected as we have previously demonstrated that vhs autoregulates its expression by various means, including the nuclear retention of its transcript, and inefficient translation of its transcript (15). Nonetheless, with its higher level of expression during HSV1 vhs-GFP infection, the GFP fusion protein allowed us to investigate vhs localization throughout the virus infection cycle. The vhs-GFP fusion protein was only detectable at 8 to 10 h after infection, at which time it localized to juxtanuclear clusters that were close to but not associated with the Golgi apparatus. As the infection progressed, fluorescence levels increased and vhs-GFP appeared throughout the cytoplasm and at the cell periphery, where it colocalized with its known binding partner, VP16. Because both vhs and VP16 were assembled into the HSV1 virion, these sites of vhs positivity were likely to represent different stages of the HSV1 morphogenesis pathway including the trafficking of structural proteins on the path to virus envelopment and the egress of enveloped virions (31).

Herpesvirus encoded endoribonucleases act by enhancing the normal rate of turnover of cellular mRNA; mRNA is first cleaved by the endoribonuclease before the cellular mRNA decay machinery acts on it (32, 33). This accelerated cleavage alters the steady-state localization of PABPC1 from cytoplasmic to nuclear as it shuttles between the nucleus and the cytoplasm (17). The most striking result from this study is that despite the lack of endoribonuclease activity and PABPC1 retention in the nucleus, vhs-GFP maintains the ability to cause the vhs-dependent nuclear retention of IE and E transcripts in WT infection. This reveals for the first time that vhs cleavage and degradation of mRNA is not a prerequisite for enhanced nuclear compartmentalization of the infected cell transcriptome. It also emphasizes that the relative steady-state localization of PABPC1 is a direct consequence of vhs endoribonuclease activity and mRNA degradation in the cytoplasm, rather than a correlate for the relative compartmentalization of the transcriptome: PABPC1 bound to the polyA tails of cytoplasmic transcripts can only return to the nucleus after mRNA degradation has released it for nuclear import (34). Much of what is known about PABPC1 compartmentalization has been elucidated from work on virus endoribonucleases, and in particular the SOX protein from Kaposi's sarcoma herpesvirus (KSHV). Similar to vhs, the activity of SOX in the cytoplasm causes the nuclear retention of both PABPC1 and mRNA (19). In the case of SOX, previous work has revealed that the inhibition of mRNA export is a direct consequence of the nuclear accumulation of PABPC1 (35). However, our results demonstrated that vhs induces the nuclear accumulation of mRNA without concomitant relocalization of PABPC1, showing that these two properties of vhs are separable and that PABPC1 accumulation in the nucleus is not a direct consequence of the increased nuclear concentration of mRNA (36).

The molecular explanation for the vhs-induced sequestration of the transcriptome in the nucleus will require further studies, but one potential explanation is that vhs causes the cytoplasmic retention of a nuclear export factor, preventing it from returning to the nucleus and thereby blocking the subsequent export of IE and E transcripts. If this is the case, then it raises the question of how L transcripts are successfully exported for the translation of structural proteins. The activities of several other virus proteins may provide clues to this. First, the IE protein ICP27 is known to be essential for late protein expression (37, 38). ICP27 is a nucleocytoplasmic shuttling protein that binds mRNA transcripts in the nucleus and helps export them in coordination with the TREX (transcription-coupled export) complex, specifically through binding to the Aly/REF factor within the complex (39, 40). ICP27 may, therefore, counteract the nuclear retention activity of vhs by bypassing the need for any specific factors retained by vhs in the cytoplasm. Interestingly, ICP27 has been shown to stimulate the translation of a subset of late HSV1 mRNAs (41), a property likely to be explained by its ability to directly bind PABPC1 and recruit it to these mRNAs (42). Additionally, deletion of either of the VP16 and VP22 components of the vhs-VP16-VP22 complex causes translational shutoff, and in the case of VP22 at least, this shutoff correlates with the entrapment of late transcripts in the nucleus (10). Hence, VP22 and VP16 quench the ability of vhs to retain the nuclear transcriptome, potentially by competing for vhs binding to specific factors in the cytoplasm, to function in coordination with ICP27 to activate late protein expression. GFP-Trap analysis of vhs-GFP expressed during infection will now provide us with the means of investigating the binding partners of vhs during infection, allowing us to investigate the full vhs interactome and identify potential candidates required for export of viral mRNAs late in infection.

These results further emphasize the role that vhs plays in regulating the antiviral response to HSV1 infection. As we have shown before, ISG transcripts are initially upregulated in HSV1 infected HFFF, before dropping again as the infection progresses, with this decrease in ISG level being dependent on vhs activity (10). Here we have shown that vhs-GFP also fails to degrade IFIT1 and IFIT2 transcripts, confirming the dependence of this process on vhs endoribonuclease activity. The PKR stress response is also upregulated in HSV1 vhs-GFP infection with a 7-fold increase in PKR phosphorylation and a 3.5-fold increase in eIF2α phosphorylation compared to WT infection, suggesting that the level of dsRNA may be increased in these infected cells. Nonetheless, there was no evidence of translational shutoff in the HSV1 vhs-GFP infected cells, indicating that the neurovirulence factor ICP34.5, which induces the dephosphorylation of eIF2α (29), is likely to counteract the increase in eIF2α phosphorylation induced by

the increased PKR phosphorylation in cells infected with virus expressing vhs-GFP. This lack of stress-induced translational shutoff is further emphasized by the fact that, despite remaining cytoplasmic in HSV1 vhs-GFP infected cells, PABPC1 did not localize to cytoplasmic foci, suggesting that recruitment of mRNA into stress granules was not a feature of this infection (43).

In combination, these results serve to further emphasize the interplay between a range of virus factors, including the dsRNA binding protein Us11 which inhibits PKR, and the neurovirulence factor ICP34.5, which reverses the phosphorylation of eiF2α and vhs, which degrades ISG transcripts and dsRNA in the antagonism of host responses to HSV infection (44). Our new virus tool that separates vhs-induced mRNA degradation from its effects on the localization of the virus transcriptome affords us a unique opportunity to investigate the relative contributions of these vhs activities to the success of HSV1 infection.

MATERIALS AND METHODS

Cells and viruses. Vero, HFFF, HaCat, and HeLa cells were cultured in Dulbecco modified Eagle's medium (DMEM) supplemented with 10% fetal bovine serum (FBS). Viruses were routinely propagated and titrated in Vero cells using DMEM with 2% FBS and supplemented with 5% human serum for titrations. The parental virus strains used in this study were HSV-1 strains Sc16 and s17. The s17-derived vhs knockout virus (Δvhs) has been described before (28). Extracellular virions were gradient purified as described previously (16). Briefly, 10 175-cm^2 flasks of confluent HaCat cells were infected at a multiplicity of 0.05. Once the cytopathic effect was advanced (3 to 4 days postinfection), the extracellular medium was collected and centrifuged at 3,000 rpm for 30 min at 4°C in a fixed-angle rotor to remove the cell debris. Virus particles were pelleted from the supernatant at 9,000 rpm for 90 min at 4°C. The particle pellet was resuspended in 0.5 mL phosphate-buffered saline (PBS) and layered onto a preformed 11 mL 5% to 15% (wt/vol) Ficoll gradient in a 13.2 mL thin-wall polyallomer ultracentrifuge tube (Beckman Coulter). Gradients were centrifuged at 12,000 rpm for 2 h at 4°C in an SW41 Ti swinging-bucket rotor in a Sorvall Discovery SE ultracentrifuge. Virions were harvested by needle puncture through the side of the tube with a 23-gauge hypodermic needle in a volume of $<$1 mL, diluted in 10 mL PBS, and pelleted at 25,000 rpm for 1 h at 4°C using the same rotor and ultracentrifuge. The pellets were resuspended in 100 μL PBS and stored at $-$80°C. Virions were solubilized in SDS-PAGE lysis buffer before analysis by SDS-PAGE and Western blotting.

Plasmids. To construct pGFP-vhs, the vhs open reading frame (UL41) was transferred from plasmid pcvhs (15) to pEGFPC1. To construct pvhs-GFP, UL41 was amplified by PCR from plasmid pGE204 (15) using primers F- GGAGATCTACATGGGTTTGTTCGGGATGA and R- GCGAATTCTCGTCCCAGAATTT and inserted into pEGFPN1. Plasmids were transfected into HeLa cells with Lipofectamine 2000.

A transfer vector to produce recombinant HSV1 vhs-GFP was constructed by amplifying the 800 bp downstream flanking region of the vhs-encoding gene UL41 from the Sc16 genome as a NotI fragment using primers F-5′CGGCGGCCGCCGTCAGACGAGCGCGCTTG3′ and R- 5′CGGCGGCCGCCGTGGCCGGTACCATCAAC3′ and inserting the amplified fragment in the NotI site downstream of GFP in pvhs-GFP.

Construction of vhs-GFP virus. Equal amounts of plasmid vhs-GFP and infectious HSV1 strain Sc16 DNA were transfected into 2 $\times$ 10^5 Vero cells grown in a well of a 12-well culture plate using lipofectamine 2000. Five days later when the cytopathic effect was extensive, the infected cells were scraped into the cell medium, subjected three times to freeze-thawing, and titrated on Vero cells. Fluorescent plaques were picked and plaque-purified a further two times before further analysis.

Antibodies. The VP22 (AGV031) antibody has been described elsewhere (29). Other antibodies used in this study were kindly provided by the following individuals: VP16 (LP1), Colin Crump (University of Cambridge); vhs, Duncan Wilson (Albert Einstein College of Medicine); TK, Frazer Rixon (Centre for Virus Research, Glasgow). Other antibodies were purchased commercially: ICP27 (Abcam); α-tubulin (Sigma), ICP5 (Virusys), PABPC1 (Santa Cruz), GFP (Clontech), PKR, eIF2α (Cell Signaling Technology), Phospho-PKR and giantin (both Abcam). Fluorescent IRDye secondary antibodies were from LI-COR.

SDS-PAGE and Western blotting. Total protein samples were analyzed by SDS-polyacrylamide gel electrophoresis (PAGE) and were either stained with Coomassie blue or transferred to a nitrocellulose membrane for Western blot analysis. Western blots were visualized on the Odyssey CLx system (LI-COR). Phosphorylated eIF2α was distinguished from eIF2α using Phos-tag SDS-PAGE (Alpha Laboratories).

GFP-TRAP pulldown assay. A GFP-TRAP agarose kit (Chromotek) was used to purify GFP-tagged protein from infected HaCat cells according to the manufacturer's instructions. Briefly, infected cells were harvested at 24 hpi, washed in d-PBS then lysed in RIPA buffer. Cell lysates were centrifuged to clear cellular debris, before mixing with dilution buffer and adding GFP-TRAP beads. At this point a modification was made to the protocol: bead binding was performed overnight rather than for 1 h. Finally, the beads were washed three times before being resuspended in 2$\times$ SDS-PAGE lysis buffer and boiled for 5 min before analysis by SDS-PAGE.

Quantitative RT-PCR (qRT-PCR). Total RNA was extracted from cells using the RNeasy plus Minikit (Qiagen). Excess DNA was removed by incubation with DNase I (Invitrogen) for 15 min at room temperature, followed by inactivation for 10 min at 65°C in 25 nM EDTA. Superscript III (Invitrogen) was used to synthesize cDNA using random primers according to the manufacturer's instructions. All qRT-PCR assays were carried out in 96-well plates using Takyon No ROX SYBR 2X MasterMix blue dTTP (Eurogentec). Primers for cellular and viral genes are shown in Table 1. Cycling was carried out in a Lightcycler (Roche), and relative expression was determined using the $\Delta\Delta$CT method (30), using 18s RNA as reference. Statistical analyses were carried out using unpaired *t* tests in GraphPad Prism 8.2.1.

TABLE 1 Primer pairs used for RT-qPCR (sequences shown 5′-3′)

Gene	Forward	Reverse
ICP22	TGTGCAAGCTTCCTTGTTTG	GGCATCGGAGATTTCATCAT
TK	TACCCGAGCCGATGACTTAC	GTTATCTGGGCGCTTGTCAT
gC	GGGTCCGTCCCCCCCAAT	CGTTAGGTTGGGGGCGCT
18s	CCAGTAAGTGCGGGTCATAAGC	GCCTCACTAAACCATCCAATCGG
IFIT1	CCTGAAAGGCCAGAATGAGG	TCCACCTTGTCCAGGTAAGT
MMP1	HP100549 (SinoBiological)	
MMP3	HP100493 (SinoBiological)	
IFIT2	PPH02853A (Qiagen)	

Immunofluorescence. Cells for immunofluorescence were grown on coverslips and fixed with 4% paraformaldehyde in PBS for 20 min at room temperature, followed by permeabilization with 0.5% Triton X-100 for 10 min. Fixed cells were blocked by incubation in PBS with 10% newborn calf serum (block buffer) for 20 min, before the addition of primary antibody in block buffer, and a further 30-min incubation. After extensive washing with PBS, the appropriate Alexafluor conjugated secondary antibody was added to the block buffer and incubated for a further 30 min. The coverslips were washed extensively in PBS and mounted in Mowiol containing DAPI. Images were acquired using a Nikon A1 confocal microscope and processed using ImageJ software (45).

Fluorescent *in situ* hybridization (FISH) of mRNA. Cells were grown in 2-well slide chambers (Fisher Scientific) and infected with the virus. At the appropriate time, cells were fixed for 20 min in 4% PFA, then dehydrated by sequential 5 min incubations in 50%, 70%, and 100% ethanol. FISH was then carried out using Applied Cell Diagnostics (ACD) RNAscope reagents according to the manufacturer's instructions. Briefly, cells were rehydrated by sequential 2 min incubations in 70%, 50% ethanol, and PBS, and treated for 30 min at 37°C with DNase, followed by 15 min at room temperature with protease. Cells were then incubated for 2 h at 40°C with RNAscope probes for virus transcripts ICP27, TK, and glycoprotein D, as designed by Advanced Cell Diagnostics, ACD, followed by washes and amplification stages according to instructions. After incubation with the final fluorescent probe, the cells were mounted in Mowiol containing DAPI to stain nuclei, and images were acquired with a Nikon A2 inverted confocal microscope and processed using Adobe Photoshop software.

Gaussia luciferase reporter assay. HeLa cells were transfected with plasmid pCMV-GLuc-1 and increasing amounts of vhs-expressing plasmids. After 16h, the medium was replaced, sampled 6 h later, and chemiluminescence measured by injection of coelenterazine at 1 μg/mL in PBS and read on a Clariostar plate reader.

ACKNOWLEDGMENTS

We thank Colin Crump, Duncan Wilson, and Frazer Rixon for the antibodies used in this study.

This work was funded by a grant from Medical Research Council, UK (MR/T0001038/1).

We declare no conflict of interest.

REFERENCES

1. Everly DN, Jr, Feng P, Mian IS, Read GS. 2002. mRNA degradation by the virion host shutoff (Vhs) protein of herpes simplex virus: genetic and biochemical evidence that Vhs is a nuclease. J Virol 76:8560–8571. https://doi.org/10.1128/jvi.76.17.8560-8571.2002.
2. Oroskar AA, Read GS. 1989. Control of mRNA stability by the virion host shutoff function of herpes simplex virus. J Virol 63:1897–1906. https://doi.org/10.1128/JVI.63.5.1897-1906.1989.
3. Elgadi MM, Hayes CE, Smiley JR. 1999. The herpes simplex virus vhs protein induces endoribonucleolytic cleavage of target RNAs in cell extracts. J Virol 73:7153–7164. https://doi.org/10.1128/JVI.73.9.7153-7164.1999.
4. Taddeo B, Roizman B. 2006. The virion host shutoff protein (UL41) of herpes simplex virus 1 is an endoribonuclease with a substrate specificity similar to that of RNase A. J Virol 80:9341–9345. https://doi.org/10.1128/JVI.01008-06.
5. Feng P, Everly DN, Jr, Read GS. 2005. mRNA decay during herpes simplex virus (HSV) infections: protein-protein interactions involving the HSV virion host shutoff protein and translation factors eIF4H and eIF4A. J Virol 79:9651–9664. https://doi.org/10.1128/JVI.79.15.9651-9664.2005.
6. Page HG, Read GS. 2010. The virion host shutoff endonuclease (UL41) of herpes simplex virus interacts with the cellular cap-binding complex eIF4F. J Virol 84:6886–6890. https://doi.org/10.1128/JVI.00166-10.
7. Doepker RC, Hsu WL, Saffran HA, Smiley JR. 2004. Herpes simplex virus virion host shutoff protein is stimulated by translation initiation factors eIF4B and eIF4H. J Virol 78:4684–4699. https://doi.org/10.1128/jvi.78.9.4684-4699.2004.
8. Smibert CA, Johnson DC, Smiley JR. 1992. Identification and characterization of the virion-induced host shutoff product of herpes simplex virus gene UL41. J Gen Virol 73:467–470. https://doi.org/10.1099/0022-1317-73-2-467.
9. Read GS, Frenkel N. 1983. Herpes simplex virus mutants defective in the virion-associated shutoff of host polypeptide synthesis and exhibiting abnormal synthesis of alpha (immediate early) viral polypeptides. J Virol 46:498–512. https://doi.org/10.1128/JVI.46.2.498-512.1983.
10. Pheasant K, Moller-Levet CS, Jones J, Depledge D, Breuer J, Elliott G. 2018. Nuclear-cytoplasmic compartmentalization of the herpes simplex virus 1 infected cell transcriptome is co-ordinated by the viral endoribonuclease vhs and cofactors to facilitate the translation of late proteins. PLoS Pathog 14:e1007331. https://doi.org/10.1371/journal.ppat.1007331.
11. Pasieka TJ, Lu B, Crosby SD, Wylie KM, Morrison LA, Alexander DE, Menachery VD, Leib DA. 2008. Herpes simplex virus virion host shutoff attenuates establishment of the antiviral state. J Virol 82:5527–5535. https://doi.org/10.1128/JVI.02047-07.
12. Dauber B, Saffran HA, Smiley JR. 2019. The herpes simplex virus host shutoff (vhs) RNase limits accumulation of double stranded RNA in infected cells: Evidence for accelerated decay of duplex RNA. PLoS Pathog 15:e1008111. https://doi.org/10.1371/journal.ppat.1008111.
13. Friedel CC, Whisnant AW, Djakovic L, Rutkowski AJ, Friedl MS, Kluge M, Williamson JC, Sai S, Vidal RO, Sauer S, Hennig T, Grothey A, Milic A, Prusty BK, Lehner PJ, Matheson NJ, Erhard F, Dolken L. 2021. Dissecting Herpes simplex virus 1-induced host shutoff at the RNA level. J Virol 95:e01399-20. https://doi.org/10.1128/JVI.01399-20.

14. Oroskar AA, Read GS. 1987. A mutant of herpes simplex virus type 1 exhibits increased stability of immediate-early (alpha) mRNAs. J Virol 61:604–606. https://doi.org/10.1128/JVI.61.2.604-606.1987.
15. Elliott G, Pheasant K, Ebert-Keel K, Stylianou J, Franklyn A, Jones J. 2018. Multiple post-transcriptional strategies to regulate the herpes simplex virus type 1 vhs endoribonuclease. J Virol 92:e00818-18. https://doi.org/10.1128/JVI.00818-18.
16. Salaun C, MacDonald AI, Larralde O, Howard L, Lochtie K, Burgess HM, Brook M, Malik P, Gray NK, Graham SV. 2010. Poly(A)-binding protein 1 partially relocalizes to the nucleus during herpes simplex virus type 1 infection in an ICP27-independent manner and does not inhibit virus replication. J Virol 84:8539–8548. https://doi.org/10.1128/JVI.00668-10.
17. Afonina E, Stauber R, Pavlakis GN. 1998. The human poly(A)-binding protein 1 shuttles between the nucleus and the cytoplasm. J Biol Chem 273:13015–13021. https://doi.org/10.1074/jbc.273.21.13015.
18. Burgess HM, Richardson WA, Anderson RC, Salaun C, Graham SV, Gray NK. 2011. Nuclear relocalisation of cytoplasmic poly(A)-binding proteins PABP1 and PABP4 in response to UV irradiation reveals mRNA-dependent export of metazoan PABPs. J Cell Sci 124:3344–3355. https://doi.org/10.1242/jcs.087692.
19. Lee YJ, Glaunsinger BA. 2009. Aberrant herpesvirus-induced polyadenylation correlates with cellular messenger RNA destruction. PLoS Biol 7:e1000107. https://doi.org/10.1371/journal.pbio.1000107.
20. Gilbertson S, Federspiel JD, Hartenian E, Cristea IM, Glaunsinger B. 2018. Changes in mRNA abundance drive shuttling of RNA binding proteins, linking cytoplasmic RNA degradation to transcription. Elife 7:e37663. https://doi.org/10.7554/eLife.37663.
21. Taddeo B, Sciortino MT, Zhang W, Roizman B. 2007. Interaction of herpes simplex virus RNase with VP16 and VP22 is required for the accumulation of the protein but not for accumulation of mRNA. Proc Natl Acad Sci U S A 104:12163–12168. https://doi.org/10.1073/pnas.0705245104.
22. Smibert CA, Popova B, Xiao P, Capone JP, Smiley JR. 1994. Herpes simplex virus VP16 forms a complex with the virion host shutoff protein vhs. J Virol 68:2339–2346. https://doi.org/10.1128/JVI.68.4.2339-2346.1994.
23. Elliott G, Mouzakitis G, O'Hare P. 1995. VP16 interacts via its activation domain with VP22, a tegument protein of herpes simplex virus, and is relocated to a novel macromolecular assembly in coexpressing cells. J Virol 69:7932–7941. https://doi.org/10.1128/JVI.69.12.7932-7941.1995.
24. Mbong EF, Woodley L, Dunkerley E, Schrimpf JE, Morrison LA, Duffy C. 2012. Deletion of the herpes simplex virus 1 UL49 gene results in mRNA and protein translation defects that are complemented by secondary mutations in UL41. J Virol 86:12351–12361. https://doi.org/10.1128/JVI.01975-12.
25. Duffy C, Mbong EF, Baines JD. 2009. VP22 of herpes simplex virus 1 promotes protein synthesis at late times in infection and accumulation of a subset of viral mRNAs at early times in infection. J Virol 83:1009–1017. https://doi.org/10.1128/JVI.02245-07.
26. Lam Q, Smibert CA, Koop KE, Lavery C, Capone JP, Weinheimer SP, Smiley JR. 1996. Herpes simplex virus VP16 rescues viral mRNA from destruction by the virion host shutoff function. EMBO J 15:2575–2581. abs.html. https://doi.org/10.1002/j.1460-2075.1996.tb00615.x.
27. Sciortino MT, Taddeo B, Giuffre-Cuculletto M, Medici MA, Mastino A, Roizman B. 2007. Replication-competent herpes simplex virus 1 isolates selected from cells transfected with a bacterial artificial chromosome DNA lacking only the UL49 gene vary with respect to the defect in the UL41 gene encoding host shutoff RNase. J Virol 81:10924–10932. https://doi.org/10.1128/JVI.01239-07.
28. Poppers J, Mulvey M, Khoo D, Mohr I. 2000. Inhibition of PKR activation by the proline-rich RNA binding domain of the herpes simplex virus type 1 Us11 protein. J Virol 74:11215–11221. https://doi.org/10.1128/jvi.74.23.11215-11221.2000.
29. He B, Gross M, Roizman B. 1997. The gamma(1)34.5 protein of herpes simplex virus 1 complexes with protein phosphatase 1alpha to dephosphorylate the alpha subunit of the eukaryotic translation initiation factor 2 and preclude the shutoff of protein synthesis by double-stranded RNA-activated protein kinase. Proc Natl Acad Sci U S A 94:843–848. https://doi.org/10.1073/pnas.94.3.843.
30. Sciortino MT, Parisi T, Siracusano G, Mastino A, Taddeo B, Roizman B. 2013. The virion host shutoff RNase plays a key role in blocking the activation of protein kinase R in cells infected with herpes simplex virus 1. J Virol 87:3271–3276. https://doi.org/10.1128/JVI.03049-12.
31. Hollinshead M, Johns HL, Sayers CL, Gonzalez-Lopez C, Smith GL, Elliott G. 2012. Endocytic tubules regulated by Rab GTPases 5 and 11 are used for envelopment of herpes simplex virus. EMBO J 31:4204–4220. https://doi.org/10.1038/emboj.2012.262.
32. Gaglia MM, Covarrubias S, Wong W, Glaunsinger BA. 2012. A common strategy for host RNA degradation by divergent viruses. J Virol 86:9527–9530. https://doi.org/10.1128/JVI.01230-12.
33. Covarrubias S, Gaglia MM, Kumar GR, Wong W, Jackson AO, Glaunsinger BA. 2011. Coordinated destruction of cellular messages in translation complexes by the gammaherpesvirus host shutoff factor and the mammalian exonuclease Xrn1. PLoS Pathog 7:e1002339. https://doi.org/10.1371/journal.ppat.1002339.
34. Burgess HM, Gray NK. 2012. An integrated model for the nucleo-cytoplasmic transport of cytoplasmic poly(A)-binding proteins. Commun Integr Biol 5:243–247. https://doi.org/10.4161/cib.19347.
35. Kumar GR, Glaunsinger BA. 2010. Nuclear import of cytoplasmic poly(A) binding protein restricts gene expression via hyperadenylation and nuclear retention of mRNA. Mol Cell Biol 30:4996–5008. https://doi.org/10.1128/MCB.00600-10.
36. Gray NK, Hrabalkova L, Scanlon JP, Smith RW. 2015. Poly(A)-binding proteins and mRNA localization: who rules the roost? Biochem Soc Trans 43:1277–1284. https://doi.org/10.1042/BST20150171.
37. Soliman TM, Sandri-Goldin RM, Silverstein SJ. 1997. Shuttling of the herpes simplex virus type 1 regulatory protein ICP27 between the nucleus and cytoplasm mediates the expression of late proteins. J Virol 71:9188–9197. https://doi.org/10.1128/JVI.71.12.9188-9197.1997.
38. Sacks WR, Greene CC, Aschman DP, Schaffer PA. 1985. Herpes simplex virus type 1 ICP27 is an essential regulatory protein. J Virol 55:796–805. https://doi.org/10.1128/JVI.55.3.796-805.1985.
39. Chen IH, Sciabica KS, Sandri-Goldin RM. 2002. ICP27 interacts with the RNA export factor Aly/REF to direct herpes simplex virus type 1 intronless mRNAs to the TAP export pathway. J Virol 76:12877–12889. https://doi.org/10.1128/jvi.76.24.12877-12889.2002.
40. Koffa MD, Clements JB, Izaurralde E, Wadd S, Wilson SA, Mattaj IW, Kuersten S. 2001. Herpes simplex virus ICP27 protein provides viral mRNAs with access to the cellular mRNA export pathway. EMBO J 20:5769–5778. https://doi.org/10.1093/emboj/20.20.5769.
41. Fontaine-Rodriguez EC, Knipe DM. 2008. Herpes simplex virus ICP27 increases translation of a subset of viral late mRNAs. J Virol 82:3538–3545. https://doi.org/10.1128/JVI.02395-07.
42. Smith RWP, Anderson RC, Larralde O, Smith JWS, Gorgoni B, Richardson WA, Malik P, Graham SV, Gray NK. 2017. Viral and cellular mRNA-specific activators harness PABP and eIF4G to promote translation initiation downstream of cap binding. Proc Natl Acad Sci U S A 114:6310–6315. https://doi.org/10.1073/pnas.1610417114.
43. Kedersha N, Stoecklin G, Ayodele M, Yacono P, Lykke-Andersen J, Fritzler MJ, Scheuner D, Kaufman RJ, Golan DE, Anderson P. 2005. Stress granules and processing bodies are dynamically linked sites of mRNP remodeling. J Cell Biol 169:871–884. https://doi.org/10.1083/jcb.200502088.
44. Zhu H, Zheng C. 2020. The race between host antiviral innate immunity and the immune evasion strategies of herpes simplex virus 1. Microbiol Mol Biol Rev 84:e00099-20. https://doi.org/10.1128/MMBR.00099-20.
45. Schneider CA, Rasband WS, Eliceiri KW. 2012. NIH Image to ImageJ: 25 years of image analysis. Nat Methods 9:671–675. https://doi.org/10.1038/nmeth.2089.